EFFECTS OF LOCAL IMMOBILE GRAVEL BED ELEVATION ON TURBULENCE

Daniel G. Wren, Research Hydraulic Engineer, USDA-ARS, Oxford, MS, Daniel.Wren@ars.usda.gov; Eddy J. Langendoen, Research Hydraulic Engineer, USDA-ARS, Oxford, MS, Eddy.Langendoen@ars.usda.gov; Roger A. Kuhnle, Research Hydraulic Engineer, USDA-ARS, Oxford, MS, Roger.Kuhnle@ars.usda.gov

Abstract Predicting sand transport over irregular substrates is difficult due to complex interactions of flow, substrate, and sediments. A better understanding of these processes is required to understand the impacts of reservoir flushing and dam removal, which both result in the introduction of finer sediments into relatively clean, coarse substrates. Modeling flow and sediment transport in these complex conditions requires an understanding of the connections between flow patterns and bed topography. An adjustable-slope, recirculating laboratory flume was used in measurements of turbulence and bed topography for a partially sand-filled immobile gravel bed with a D_{50} of 35 mm. Detailed flow measurements were made using an acoustic Doppler velocimeter that measured three velocity components at a rate of 200 Hz. The response of turbulence to local gravel bed roughness was investigated using visual and statistical measures of the connection between local bed elevations and Reynolds stresses. Gravel elevations were averaged over wall-parallel strips 1-20 cm in length and 3.5 cm (about one D_{50}) in width. Mean elevations over shorter lengths were negatively correlated with near-bed Reynolds stress, and longer regions were positively correlated for $z/h>0.2$ where z is elevation and h is the water depth. The relationship between the standard deviation of gravel elevation and Reynolds stress was much weaker than for mean elevation.

INTRODUCTION

The interaction of a coarse stream bed with flow and sediment is complex, and the controlling factors, such as bed roughness, slope, and availability of fine sediments, are difficult to measure. However, planning for reservoir flushing or dam removal requires knowledge of such interactions. In both cases, sediment may be reintroduced to beds that have had fine particles removed without replacement from upstream, leaving pore space which interacts with the flow and represents available storage capacity. The proportion of a gravel bed stream that is covered by sand strongly affects generation of turbulence and, hence, the amount of sediment transported. The relationship between bed coverage, transport rate, and bed shear stress is poorly understood (Grams and Wilcock, 2007).

Many previous studies of turbulence over rough beds have focused on the effects of isolated roughness, such as those imparted by clusters or micro-clusters which that have greater elevation than their surroundings (Strom and Papanicalou, 2007; Strom et al., 2003; Buffin Belanger and Roy, 1998). In the present work, randomly placed immobile gravel did not develop discernable clusters, which allowed examination of the evolution of turbulent shear stress on a uniform rough bed in the presence of suspended-sediment. The results of turbulence and topography measurements over an immobile gravel bed filled with sand to within approximately 2.7 cm of the maximum gravel elevation are reported.

METHODS AND MATERIALS

The experiments were carried out at the United States Department of Agriculture-Agricultural Research Service-National Sedimentation Laboratory in a 15-m (L) x 0.36-m (W) x 0.46-m (D) sediment and water recirculating flume with adjustable slope and a frequency-controlled motor. The bed of the flume was covered with gravel ($D_{50} = 35$ mm) randomly deposited to a mean depth of approximately 17.5 cm (maximum 19.5 cm) and screeded flat. Sand (D_{50}=0.3 mm) was also present in the bed (Figure 1).

Water surface slope was measured by an acoustic sensor that traversed the length of the flume along its centerline. Discharge, Q, was obtained from a calibrated venturi meter in the return line. Depth-integrated flow velocity was found using $\bar{U} = Q/A$, where A is the cross-sectional area of the flowing water. Mean water depth, h, was measured during each experiment using acoustic probes to identify the water surface and bed surface elevations. Froude number, Fr, was determined from $Fr = \bar{U}/\sqrt{gh}$, where g is the acceleration due to gravity. Wall corrected bed shear stress was determined from $\tau_0 = \rho g h S$, where ρ is fluid density. The wall correction was

based on modifications of the Vanoni and Brooks (1957) method as described in Vanoni (1975) with further modification by Chiew and Parker (1994), which resulted in an explicit relationship for wall friction.

The coordinate system used in the study was as follows: *X*=streamwise direction and *u*=streamwise velocity, positive away from datum at flume entrance; *Y*=cross-stream direction and *v*=cross-stream velocity, positive away from datum at right flume wall facing downstream; and *Z*=vertical direction and *w*= vertical velocity, positive up from the datum at the flume floor.

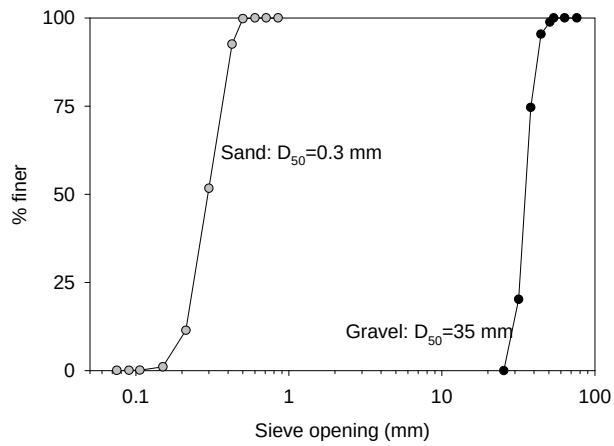

Figure 1 Grain size distribution for gravel and sand used in flume.

An acoustic Doppler velocimeter (Nortek Vectrino) was used to measure fluid velocity and turbulence. The Vectrino used a 10 MHz beam to ensonify a region of the flow approximately 5 cm below the sensor head and collected velocities in the *X*, *Y*, and *Z* directions. The sampling volume was a cylinder 6 mm in diameter and 7 mm tall, resulting in a measurement volume of approximately 200 mm^3. A 2-minute sampling period was chosen to adequately characterize the mean and turbulent quantities while maintaining a time period feasible for collecting detailed grids of velocity data. A three-dimensional axis system was used to move the velocity probe over a 252 point grid with the following dimensions: *X*=20 cm, *Y*=10 cm, and *Z*=7 cm. The data were arranged into 6 planes (42 points each) parallel to the bed with elevations of *Z*=0, 1, 2, 3, 5, and 7 cm above an origin that approximately coincided with the mean gravel elevation. Data were collected at *Y*=8, 10, 12, 14, 16 and 18 cm from the right flume wall. The most upstream sampling location was 11.8 m from the flume entrance, and data were collected 0, 3, 6, 10, 13, 16, and 20 cm downstream from there.

Images of the bed surface were used to generate digital elevation maps (DEM) of the gravel topography. The photos were taken with a Pentax K10D digital camera with a Pentax P-DA 18-55 mm F3.5-5.6 lens. This camera had a maximum image size of 3872×2592 pixels (10MP). The camera was mounted on a carriage that traversed the top of the flume. After acquiring the images, the camera was calibrated on a checkerboard pattern following the procedure of Bouguet (2008) to determine the intrinsic camera parameters and lens distortion. To minimize the error in these parameters, the calibration images covered the entire range in angles (0-90°) and azimuths (0-360°). Adobe Photoshop® was used to convert both calibration and 3D reconstruction images to PNG format, which uses a lossless compression algorithm. Camera intrinsic parameters and lens distortion parameters were determined using the Matlab® Camera Calibration Toolbox (Bouguet, 2008). The 3D reconstruction images were then undistorted using the derived intrinsic and distortion parameters. The undistorted reconstruction images were then processed using ERDAS LPS ® v9.3 (Leica Geosystems, 2002). Using corresponding control points and features (tie points) in an image pair, ERDAS LPS triangulates the position and orientation of the camera (known as external camera parameters) for each image. The triangulation was performed on the complete set of images using a bundle block adjustment technique. Because the system of unknown parameters (camera external parameters and tie point world coordinates) is overdetermined, this technique uses least-square adjustment to minimize the error in the solution. The DEM was then extracted with the obtained camera external parameters and the matching area in an image pair. The resulting DEMs have a horizontal resolution of about 15 pixels (~1.5 mm).

The sand elevation relative to the maximum gravel elevation, Z_s, was defined to be zero when the mean sand elevation was the same as the maximum gravel elevation, with Z_s taking on negative values when the sand elevation was below that of the gravel and positive values when the sand elevation was above the gravel. A volumetric approach was taken for estimating Z_s. It was assumed that each volume increment of sand was uniformly distributed over the length of the flume. The volume of sand was based on known mass and assumed porosity of 0.4. The increasing porosity of the top layer of gravel was unknown, and therefore was measured so that it could be used to calculated sand elevations. The work reported here was all collected for Z_s =-2.7 cm. At this sand elevation, there was little sand visible in the gravel, allowing the elevation of the immobile gravel bed from the DEM to be used for the entire period of Vectrino data collection. Since it was not feasible to collect continuous records of bed elevation, this particular analysis could not be undertaken with sand waves changing surface characteristics through the data collection period.

Processing velocity data

Mean velocities were calculated from filtered Vectrino data as follows:

$$U = \frac{1}{T}\sum_{i=1}^{n} u_i \Delta t_i \quad , \quad W = \frac{1}{T}\sum_{i=1}^{n} w_i \Delta t_i \tag{1}$$

where T=total time, Δt =time increment, n=total number of measurements, and u_i and w_i are single velocity measurements. Reynolds stresses were calculated from

$$\tau_{\mathrm{Re}} = -\rho \overline{u'w'} \tag{2}$$

where $u_i' = u_i - U$ and $w_i' = w_i - W$. Turbulence intensities were calculated from:

$$u_{\mathrm{rms}} = \sqrt{\frac{1}{n}\sum_{i=1}^{\mathrm{n}} \left(u_i - U\right)^2} \quad \text{and} \quad w_{\mathrm{rms}} = \sqrt{\frac{1}{n}\sum_{i=1}^{\mathrm{n}} \left(w_i - W\right)^2} \quad . \tag{3}$$

The Vectrino data were filtered in a two-stage process. First, the data in beam coordinates were despiked with no replacement using a progressive threshold of 3.3, 3.6, and 4.3 times the standard deviation of each time series. Second, the data were transformed into orthogonal components and despiked with no replacement using the universal threshold $\mathrm{UT} = \sigma\sqrt{2\ln n}$, where σ=standard deviation (Goring and Nikora, 2002). All despiking was implemented in multiple passes until the standard deviation in subsequent passes differed by less than 0.005. This step prevented excessively large threshold values caused when a small number of large outliers resulted in a high value for σ, allowing spurious data to remain in the time series. For a single sampling location to be included in a profile, the time series was required to have $n_{\mathrm{points}} > 17,000$.

Other methods for filtering the data, such as those described by Hurther and Lemmin (2001), Goring and Nikora (2002), and Franca and Lemmin (2006), were applied to the data. However, these methods provided less satisfactory results than that described above. As a check on the data processing technique, the turbulence spectra were examined. Both Figure 2a (z/h=0.05) and Figure 2b (z/h=0.33) show clearly that the decreasing energy trend in the power spectral densities of the unfiltered data flattened out at frequencies larger than 5 Hz. The despiked data continue to decrease in power down to near the Nyquist frequency of 100 Hz before flattening slightly. As shown in both figures, the rate of energy decay approximates the expected $-5/3$ slope based on the theory of Kolmogorov (Schlichting, 1968).

Strom and Papanicolaou (2007) discuss several strategies for filtering data from acoustic velocimeters. One of them is to ensure that the data adhere to accepted theory and expected patterns of change with depth. The present data set fit the expected downstream and vertical distribution of relative turbulence intensity as defined by Nezu and Nakagawa (1993) and resulted in bed shear stress estimates that, although they varied from those obtained using the

depth-slope product, exhibited a generally consistent offset from the bulk flow derived stress estimate as well as expected decreases with decreasing roughness.

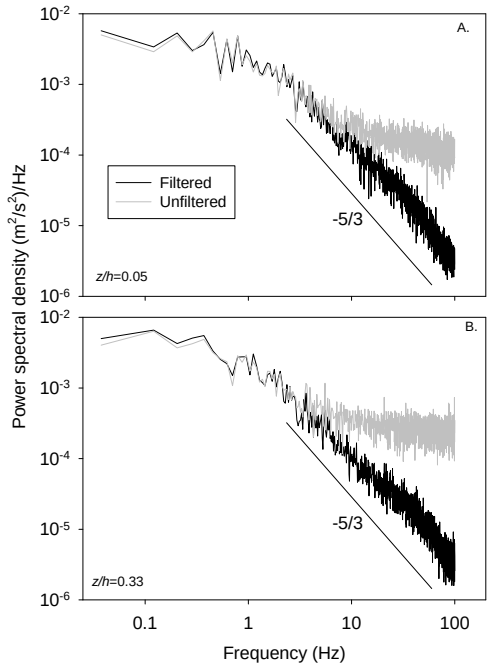

Figure 2 Turbulence spectra for filtered and unfiltered downstream velocity data for 50 l/s and Z_s=-2.1 cm at (A.) z/h=0.05 and (B.) z/h=0.33.

RESULTS

The gravel elevation data obtained through stereophotogrammetry is shown along with the positions of the 42 velocity profiles in Figure 3. The *X*-origin for Figure 3 coincides with the most downstream line of sampling positions, with *X* increasing in the upstream direction. Each label contains the *X*-*Y* coordinates of the position. The mean elevation of the gravel relative the flume bottom was 17.5 cm. The lowest level of Vectrino data collection, designated as 0 cm elevation, was at approximately the same elevation at 17.2 cm. The majority of the gravel elevations were within ±2 cm of the mean elevation.

Figures 4 and 5 show contour maps of sidewall parallel strips of gravel topography directly upstream of measurement positions, along with associated flow and turbulence data. Velocity profiles were collected in seven streamwise positions which are designated in the line plots and contour map. Mean downstream velocities in Figures 4A and 5A show only weak dependence on local gravel topography, as indicated by the small spread of data near the bed. In figures 4B, 4C, 5B, and 5C, turbulence intensities have more spread in the near-bed data, showing the effect of turbulence generation from variable bed roughness. The Reynolds stresses in 4D and 5D show the greatest effect from local roughness, as should be expected based on the turbulence intensities. Because the Reynolds stress is relatively more sensitive to bed topography, the remaining discussion will focus on how Reynolds stresses respond to changes in bed elevation and roughness. The Reynolds stresses trended increased with distance from the water surface, until beginning to decrease 2-3 cm above the bed (Figures 4D and 5D). One effect of local topography that is also clear in Figures 4D and 5D is a tendency for Reynolds stress to decrease downstream of locally high elevations. This can be seen in the *X*=4 and *X*=0 data in Figure 4D as well as in X=4 and X=7 data from Figure 5D. These decreases are most pronounced at *Z*=1 cm, with Reynolds stress at times increasing again at the lowest elevation as seen for *X*=4 in Figure 4D and *X*=4 and *X*=0 in Figure 5D. It is likely that these decreased Reynolds stress values are indicative of disorganized motion caused by separated flow in the wake of upstream gravel particles, much like the decreased Reynolds stresses observed in the wake of sand dunes (Wren et al., 2007; Venditti and Bennett, 2000).

The mean elevation profile for each 35 mm wide strip of gravel is shown in Figures 4F and 5F. Since the Vectrino data were collected using a fixed grid, some near-bed measurements coincided with gravel particles that were well above the mean elevation. This is clear in Figure 4F, where the Vectrino sampling volume at *X*=7 and *X*=10 was below the local gravel level, resulting in no data for those points. The 10 cm position in Figure 5F shows the same result. The mean elevation profile in Figure 5F also appears to also have been collected over a particle, but the topography in Figure 5E shows that, although the mean elevation was higher than the sampling volume, the local gravel elevation was between 0 and -0.4 cm below the sampling volume. This shows the value of detailed three dimensional gravel topography for the study of bed/turbulence interaction.

The relationship between local topography and Reynolds stress observed in Figures 4 and 5 prompted a more in-depth quantitative investigation of topography and Reynolds stress at all 42 sampled positions. Figure 6A shows the correlation between the mean upstream elevation and Reynolds stress. Elevations were calculated over 37 mm cross-stream strips that extended from 0-20 cm upstream of the sampling volume. Correlations were calculated for each of the 6 elevations at which Vectrino data were collected. Figure 6B shows the P-value, which tests the hypothesis of no correlation. Each P-value is the probability of getting a correlation as large as the observed value by random chance, when the true correlation is zero. If $P<0.05$, the correlation is considered to be significant. Figure 6A shows that the correlations for elevations *Z*=0-3 were poorly correlated 0-4 cm upstream, with magnitudes of negative correlation increasing up to a point, then decreasing. The length of upstream area best correlated with Reynolds stress increased with elevation through *Z*=3 cm. For *Z*=0, the strongest correlation was for the average elevation over an area approximately 7-8 cm upstream; for *Z*=1 it was 7-9 cm; for *Z*=2, 10-11 cm; and for *Z*=3, 16-18 cm. For *Z*=5 and 7 cm, correlations were weak and positive, and the P-values indicate that the correlations at *Z*=5 and 7 were not significant, except for possibly the 9 cm strip at *Z*=7, where P=0.054. As mentioned in the discussion accompanying Figures 4 and 5, the likely explanation for the negative correlation with upstream elevation is separation caused by locally high elevations of gravel particles. The greater length of upstream strip associated with changes in Reynolds stress for $Z\geq5$ may be explained by the propagation of bed-generated turbulence up from the bed. The flow at *Z*=5 and 7 cm is unlikely to be affected by the bed just upstream because the intervening distance is too small for the turbulence to be advected up from the bed to that elevation.

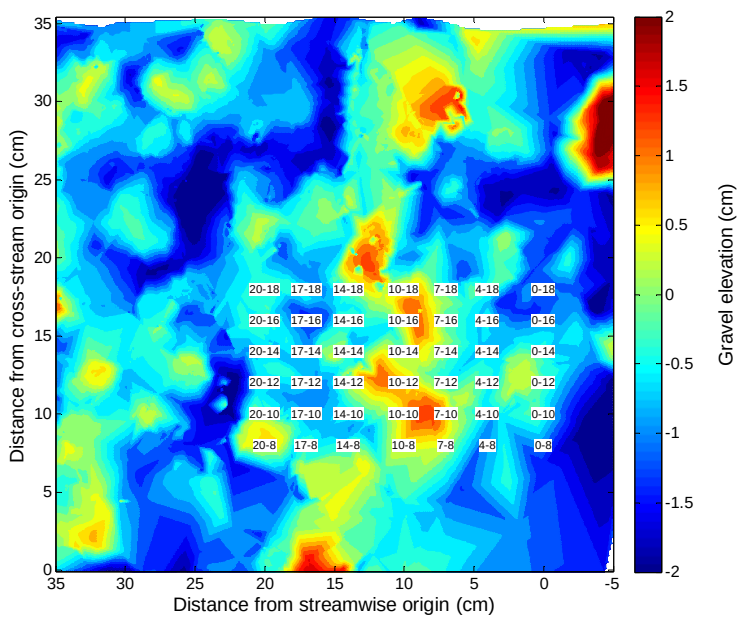

Figure 3 Gravel elevations and positions for velocity profiles. Flow is from left to right.

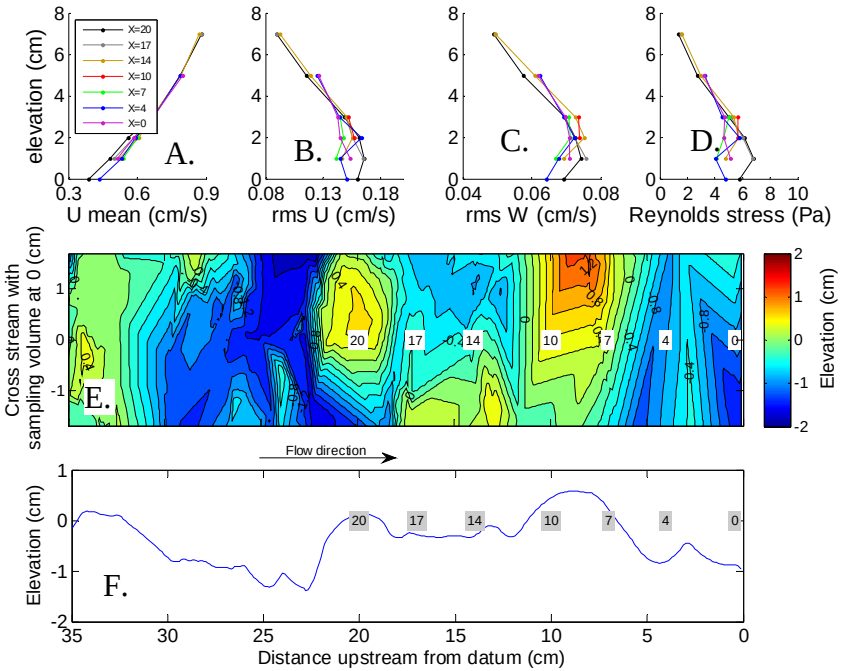

Figure 4 Downstream velocity, rms U, rms W, and Reynolds stress over a strip of gravel bed 8 cm from the flume sidewall for sand elevation of -2.7 cm relative to the gravel and a discharge of 50 l/s. The center of the numbered squares in the contour plot represent the location of the sample volume of the Vectrino and correspond to the X coordinates in the legend of the U mean data. The elevations in the profile plot are means across the 3.5 cm wide upstream strip.

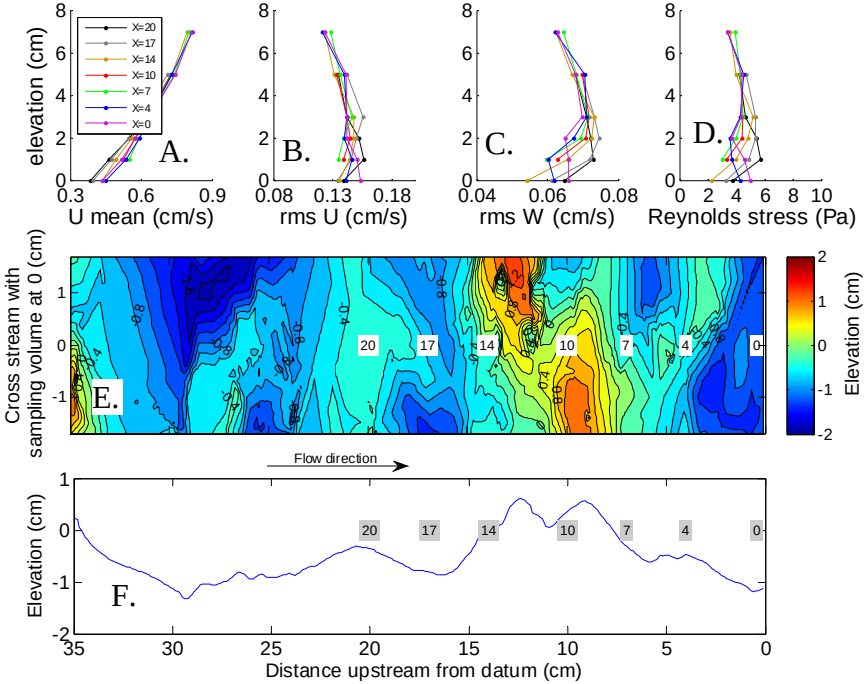

Figure 5 Downstream velocity, rms U, rms W, and Reynolds stress over a strip of gravel bed 18 cm from the flume sidewall for sand elevation of -2.7 cm relative to the gravel and a discharge of 50 l/s. The center of the numbered squares in the contour plot represent the location of the sample volume of the Vectrino and correspond to the X coordinates in the legend of the U mean data. The elevations in the profile plot are means across the 3.5 cm wide upstream strip.

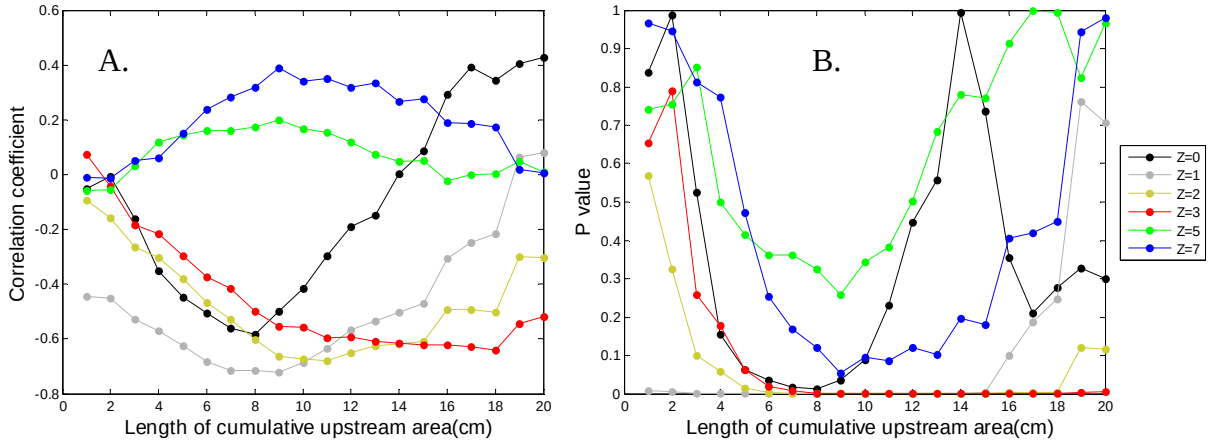

Figure 6 (A.) Correlation and (B.) P-Value for Reynolds stress and average gravel elevations calculated for areas 37 mm wide with length specified on the X-axis. Each point on the plot represents the correlation between the set of Reynolds stresses and mean upstream gravel elevation. The P-value is the probability of getting a correlation by random chance if the true correlation is zero. Here, P<0.05 was taken as significant.

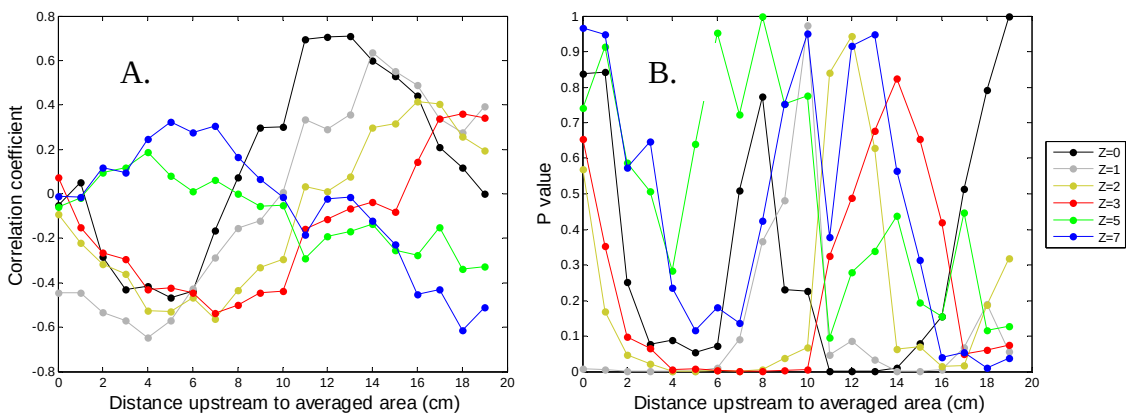

Figure 7 (A.) Correlation and (B.) P-Value for Reynolds stress and average gravel elevations calculated for areas 37 mm wide separated from the sampling volume by upstream distance specified on the X-axis. Each point on the plot represents correlation between the set of Reynolds stresses and upstream gravel elevation. The P-value is the probability of getting a correlation by random chance if the true correlation is zero. Here, P<0.05 was taken as significant.

Figure 7 differs from Figure 6 in the treatment of the area over which the gravel elevation was averaged. The areas in Figure 6 included all gravel elevations within strips of various lengths. In Figure 7, the areas are all one cm in streamwise extent and are separated from the sampling volume by the distance specified on the *X*-axis. The correlations in Figure 7 are significant for *Z*=0 at streamwise separations of 11-14 cm (-); for *Z*=1: 0-5 cm (-) and 14-16 cm (+); for *Z*=2: 3-9 cm (-) and 16-17 cm (+); for *Z*=3: 5-10 cm (-), for *Z*=5: none; and for *Z*=7: 16 (-) and 18-19 cm (-). There is a general trend towards negative correlation at low elevations, moving through weak correlation to positive correlation with increasing upstream distance. Reynolds stresses for *Z*≥5 cm had the opposite trend, with positive correlation to nearby mean gravel elevation moving to negative correlation with increasing separation from the sampling volume. The generally weaker correlations with mean elevation for separated areas compared to cumulative areas may be explained by the cumulative effect of fluid interacting with the bed. It should be expected that this would be the case; however, the significant correlation of Reynolds stress and mean elevation of separated upstream areas was not expected. The connection may be due to the relatively small range of variability in the gravel elevation (-2<*Z*<2 cm) and the repetitive nature of the bed topography caused by the small range in gravel particle size.

Correlations and P-values for Reynolds stress and the standard deviation of the elevations for the upstream area are shown in Figure 8A and 8B. The behavior is very different from that seen for correlations between mean upstream elevation and Reynolds stress. Near bed Reynolds stresses are weakly positively correlated, with P-values indicating no significant correlation except for *Z*=0 at 4-5 cm. Significant negative correlations were found for *Z*=5 and *Z*=7 for areas extending 8-9 cm upstream. The strong influence of high mean upstream elevations may account for the weak connection with the standard deviation of elevations. Since it is likely that separated flow from these elevated areas is the cause of lowered Reynolds stresses downstream, it is reasonable to expect that variability in elevation would have less effect. Areas with elevations below the mean may have significant variability in elevation that has only a relatively small effect on downstream turbulence.

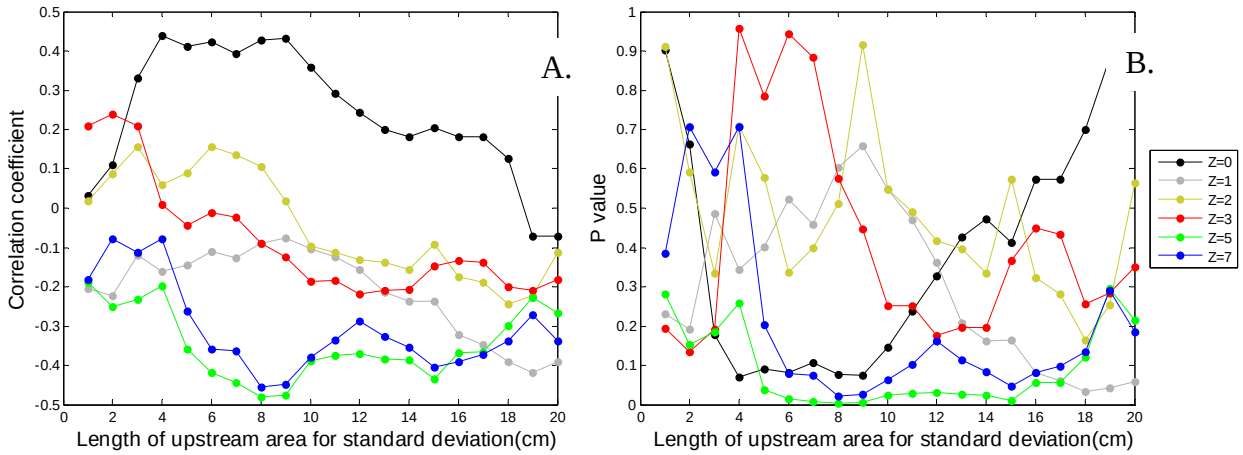

Figure 8 (A.) Correlation and (B.) P-Value for Reynolds stress and the standard deviation of gravel elevations calculated for areas 37 mm wide with length specified on the X-axis. Each point on the plot represents the correlation between the set of Reynolds stresses and upstream gravel standard deviations. The P-value is the probability of getting a correlation by random chance if the true correlation is zero. Here, P<0.05 was taken as significant.

CONCLUSIONS

Flow and turbulence data were analyzed along with upstream bed topography to assess the connection between local topography and turbulence, specifically Reynolds stress. Profiles of mean flow and turbulence were collected over a gravel bed using an acoustic Doppler velocimeter, and bed topography was measured using stereophotogrammetry. Profiles of downstream velocity and turbulence quantities were plotted in relation to sampling position in the local bed maps, allowing the broad trend of decreasing Reynolds stress downstream from topographic high points to be observed. The randomly placed immobile gravel allowed the evolution of turbulent shear stress on a uniform rough bed in the presence of suspended-sediment to be examined, in contrast to previous work which has focused on the effects of isolated roughness, such as clusters or micro-clusters that are rougher than their surroundings. Further quantitative analysis of the relationship between bed topography and flow yielded the following conclusions:

- Negative correlations between mean bed elevation and Reynolds stresses varied by elevation, with higher elevations more strongly correlated with longer sections of the bed:
    - At Z=0 cm, the strongest negative correlation was with a 7-8 cm strip
    - At Z=1 cm, the strongest negative correlation was with a 7-9 cm strip
    - At Z=2 cm, the strongest negative correlation was with a 10-11 cm strip
    - At Z=3 cm, the strongest negative correlation was with a 16-18 cm strip
    - At Z=5 and 7 cm, correlations were positive, but not significant (P>0.05)
- The mean elevation of separated upstream areas had a weaker connection to Reynolds stress, reflecting the cumulative nature of flow/bed interaction.
    - The trend was towards negative correlation for low elevation Reynolds stresses, moving through weak correlation to positive correlation with increasing upstream distance.

  - Reynolds stresses for $Z \geq 5$ cm had the opposite trend, with positive correlation to nearby mean gravel elevation moving to negative correlation with increasing separation from the sampling volume.
- Weak relationships between the standard deviation of upstream gravel elevation were observed in most cases. However, some significant relations were found.
  - At Z=1 cm, there was significant negative correlation for areas 18-19 cm
  - At Z=5 cm, there was significant negative correlation for areas 5-17 cm
  - At Z=7 cm, there was significant negative correlation for areas 8-9 cm

These conclusions show how far upstream one must look to find the features that create the turbulence measured at a given location for the conditions of these experiments. This value can impact the selection of cell size in future numerical simulations of bed/fluid interaction as well as contributing to the general understanding of turbulence generation and flow interaction with rough or porous beds.

REFERENCES

Bouguet, J.-Y. (2008), "Camera calibration toolbox for Matlab®." http://www.vision.caltech.edu/bouguetj/calib_doc/index.html, Accessed on July 2, 2008.

Buffin Belanger, T., and Roy, A. G. (1998), "Effects of a pebble cluster on the turbulent structure of a depth-limited flow in a gravel-bed river." *Geomorphology*, 25, 249-267.

Chiew, Y. and Parker, G. (1994), Incipient motion on non-horizontal slopes, *Journal of Hydraulic Research*, 32(5), 649-660.

Franca, M. J. and Lemmin, U. (2006), Eliminating velocity aliasing in acoustic Doppler velocity profiler data, *Meas. Sci. Technol.* 17, 313-322.

Goring, D. G. and Nikora,V. I. (2002), Despiking acoustic Doppler Velocimeter data, *Journal of Hydraulic Engineering*, 128(1), 117-126.

Grams. P. E. and Wilcock, P. R. (2007), Equilibrium entrainment of fine sediment over a coarse immobile bed, *Water Resources Research*, 10.1029/2006WR005129.

Hurther, D. and Lemmin, U. (2001), A correction method for turbulence measurements with a 3D acoustic Doppler velocity profiler. *Journal of atmospheric and oceanic technology*. 18, 441-458.

Leica Geosystems (2002). IMAGINE OrthoBASE User's Guide. Leica Geosystems, GIS & Mapping Division, Atlanta, GA, 508 pages.

Nezu, I., and Nakagawa, H. (1993), Turbulence in Open Channel Flows, Balkema, Rotterdam, The Netherlands.

Schlichting, H. (1968). Boundary-layer theory, McGraw-Hill, New York.

Strom, K., Papanicolaou, A. N., Evangelopoulos, N., and Odeh, M. (2003). "Microforms in grvel bed rivers: Formation, disintegration and effects on bedload transport." *Journal of Hydraulic Engineering*, 130(6), 554-597

Strom, K. B. and Papanicolaou, A. N., (2007), ADV measurements around a cluster microform in a shallow mountain stream, *Journal of Hydraulic Engineering*, 133(12), 1379-1389.

Vanoni, V. A. (1975), Sedimentation Engineering, ASCE Manual #54, New York.

Vanoni, V. A., and Brooks, N. H. (1957). Laboratory Studies of the Roughness and Suspended Load of Alluvial Streams. Sedimentation Laboratory Report No. E68. California Institue of Technology, Pasadena, CA. Vericat, D., Batalla, R. J., and Gibbins, C. N. (2008), Sediment entrainment and depletion from patches of fine material in a gravel-bed river, *Water Resources Research*, 10.1029/2008WR007028.

Venditti, J. G. and Bennett, S. J., (2000), Spectral analysis of turbulent flow and suspended sediment transport over fixed dunes, *Journal of Geophysical Research.*, 105(C9):22,035-22,047.

Vericat, D., Batalla, R.J. and Gibbins, C.N. (2008). Sediment entrainment and depletion from patches of fine material in a gravel-bed river. *Water Resources Research*. Vol. 44, W11415.

Wren, D. G., Kuhnle, R. A., and Wilson, C. G. (2007), Measurements of the Relationship between Turbulence and Sediment in Suspension over Mobile Sand Dunes in a Laboratory Flume, *Journal of Geographical Research-Earth Surface.* 112, F03009, doi:10.1029/2006JF000683.